ELSEVIER

Biomaterials 23 (2002) 3749–3756

Biomaterials

www.elsevier.com/locate/biomaterials

In vitro behavior of silicate glass coatings on Ti6Al4V

E. Saiz[a], M. Goldman[a], J.M. Gomez-Vega[a], A.P. Tomsia[a,*], G.W. Marshall[b], S.J. Marshall[b]

[a] *Lawrence Berkeley National Laboratory, Materials Sciences Division, MS 62-203 1 Cyclotron Road, Berkeley, CA 94720, USA*
[b] *University of California, Department of Restorative Dentistry, San Francisco, CA, USA*

Received 8 October 2001; accepted 14 March 2002

Abstract

The in vitro response in simulated body fluid (SBF) of silicate glass coatings on Ti6Al4V was evaluated. Glasses belonging to the SiO_2–CaO–MgO–Na_2O–K_2O–P_2O_5 system were used to prepare 50–70 μm thick coatings on Ti6Al4V, employing a simple enameling technique. Glasses with silica content higher than 55 wt% can be used to prepare coatings that do not crack or delaminate and exhibit good adhesion to the alloy. It has been found that coatings with silica content lower than 60 wt% are more susceptible to corrosion and precipitate carbonated hydroxyapatite on their surface during in vitro tests. However, these coatings have a higher thermal expansion than the metal and are under tension. After 2 months in SBF cracks grow in the coating that reach the glass/metal interface and initiate delamination. Glasses with silica content higher than 60 wt% are more resistant to corrosion and have lower thermal expansion. These coatings do not crack but they do not precipitate apatite even after 2 months in SBF.

Keywords: Coatings; Glass; Ti6Al4V; Hydroxyapatite; In vitro

1. Introduction

Titanium and Co–Cr alloys are the most popular choices for fabrication of orthopedic implants where high strength is required. These alloys exhibit good mechanical properties but are bioinert and attach to the bone through form fit or frictional connections. The weak bone to implant adhesion can result in implant loosening and failure. Coating the metallic implants with bioactive layers allows biological interaction between the bone and the implant and can consequently improve adhesion. Furthermore, the coatings could protect the implants from corrosion, limiting the release of metallic ions into the body [1–4].

In previous work, we reported the development of bioactive coatings using a new family of glasses in the SiO_2–Na_2O–K_2O–CaO–MgO–P_2O_5 system [5–7]. The glasses are based on Hench's Bioglass® and have silica contents ranging from 44 to 70 wt%. Coatings on Ti and Ti6Al4V were successfully fabricated using glasses whose silica content was >55%. At lower silica contents, the coatings cracked due to the high stresses that result from the large difference in thermal expansion between the glasses and the alloys.

In vitro tests in cell-free solutions with ionic concentrations similar to those of body fluids allow analysis of the chemical and microstructural evolution of the coatings under conditions that simulate their biological interactions with the body. Because the solution-precipitation processes that occur on the coating surfaces have a determinant role on their bone bonding mechanisms, studies in simulated body fluid (SBF) provide fundamental data to predict and understand the in vivo behavior and long-term stability [8,9]. The purpose of the present work is to systematically evaluate the in vitro behavior of the silicate glass coatings on Ti6Al4V. The study focuses on the ability of the coatings to precipitate apatite (the mineral component of the bone) and the effects of long-term immersion in SBF on the coating adhesion to the metal.

2. Experimental

The starting glasses were prepared using a conventional procedure. The appropriate reagents (SiO_2

*Corresponding author. Tel.: +1-510-486-4918; fax: +1-510-486-6086.
E-mail address: aptomsia@lbl.gov (A.P. Tomsia).

0142-9612/02/$ - see front matter
PII: S0142-9612(02)00109-6

(99.5%, purity),[1] $CaCO_3$ (99.9%),[2] MgO (98.6%),[2] K_2CO_3 (99%),[3] $NaHCO_3$ (99.5%)[2] and $NaPO_3$ (99.7%)[3]) were mixed in ethanol using a high-speed stirrer. The mixture was first dried at 80°C for 12 h and then fired in air at temperatures ranging between 1400°C and 1500°C for 4 h in a Pt crucible. The melt was cast into a graphite mold to obtain glass plates ($\sim 50 \times 50 \times 5\,mm^3$) that were subsequently milled in a planetary agate mill. In order to prepare the coatings, a suspension of the glass powder (particle size $< 20\,\mu m$) in ethanol was deposited on Ti6Al4V plates (99.0% purity, $15 \times 10 \times 1\,\mu m^3$), which had been previously polished with diamond (1 mm particle size) and cleaned in acetone and ethanol. Afterwards, the coatings were dried in air at 75°C overnight and fired at temperatures ranging between 800°C and 820°C for 30 s in order to make the glass flow and adhere to the metal [5–7]. The compositions of the coatings are shown in Table 1 (in the glass designation the number after 6P corresponds to its silica content in wt%). The coatings exhibited good adhesion to the alloy (they did not delaminate during interfacial indentation tests) and their final thickness ranged between 50 and 70 μm [5,7].

The in vitro response of the coatings was studied by immersing the specimens ($10 \times 10\,mm^2$ area) in 20 ml of SBF (Table 2) at 36.5°C for fixed periods of time up to 2 months. The solution was buffered at the physiological pH 7.25 at 36.5°C with 50 mM trishydroxymethyl aminomethane [$(CH_2OH)_3CNH_2$] and 45 mM hydrochloric acid (HCl). In order to analyze the effect of the amount of SBF, the same tests were repeated using 200 ml of SBF. The role of the calcium ions in the solution was analyzed by conducting in vitro tests in a solution having identical composition of SBF and buffered the same way, but without Ca^{2+} (Table 2). After the required times, the samples were removed from the liquid, rinsed in distilled water and dried with an air gun. Inductively coupled plasma (ICP) analysis was performed on the remaining SBF to monitor the concentrations of Ca, P, Si, and Mg. After drying, the coating surfaces and polished cross sections (up to 1 μm diamond) were analyzed by X-ray diffraction (XRD), atomic force microscopy (AFM), X-ray photoemesion (XPS), scanning electron microscopy with associated calibrated energy dispersive analysis (SEM-EDS) and Fourier Transform Infrared Spectromicroscopy (FTIRSM) in the Advanced Light Source (ALS) at Lawrence Berkeley National Laboratory. The contact AFM analysis was carried out using a Park M5 instrument (Park Scientific Instruments) using the constant force mode and Ultralever silicon tips from Park. The XPS analysis was performed on a Physical Electronics PHI 5400 ESCA using an Mg anode as an X-ray source. The SEM analysis was performed on a DS130C microscope (Topcon) and the EDS analysis was done using a DX-4 system (EDAX). Prior to the EDS analysis the samples were coated with a thin carbon layer and the system was calibrated using glasses and calcium phosphates of known composition. The accelerating voltage was 15 kV, resulting in a spot size of $\sim 1\,\mu m$. The FTIRSM uses the synchrotron beam at the ALS as an external light source in a Nicolet Magna 760 bench with Nic-Plan IR Microscope, which allows focusing the beam in very small diameters with little loss of signal. With a $32\times$ objective, the full-width half-maximum spot size is ~ 10 μm; this spot size becomes diffraction limited at longer wavelengths. The spectra were taken in the reflectance mode using a KBr beam splitter and a mercury cadmium telluride detector.

Crack growth in the coatings, when immersed in SBF, was analyzed by following the evolution of well-defined cracks generated by Vickers indentations (1.2 kg load) on the coating surfaces. Crack growth was followed by immersing the indented samples in SBF or dehydrated mineral oil at 36.5°C and measuring the crack lengths after selected times up to 8 days using optical microscopy. A qualitative test of adhesion between the coatings and the metals after immersion in SBF was performed using Vickers indentations at the glass/metal interfaces on polished cross sections with loads ranging from 0.05 to 1.2 kg in air and SBF, and analyzing the relative crack resistance [5].

Table 1
Compositions and thermal expansion of the glasses used in the preparation of the coatings analyzed in this work (in wt %)

	SiO_2	Na_2O	K_2O	CaO	MgO	P_2O_5	α ($°C^{-1}$)
Bioglass®	45.0	24.5		24.5		6.0	15.1
6P57	56.5	11.0	3.0	15.0	8.5	6.0	10.8
6P61	61.1	10.3	2.8	12.6	7.2	6.0	10.2
6P68	67.7	8.3	2.2	10.1	5.7	6.0	8.8

Table 2
Ion concentrations of the solutions used in this research and of human plasma.

	Ion concentration (mM)							
	Na^+	K^+	Ca^{2+}	Mg^{2+}	Cl^-	HCO_3^-	HPO_4^{2-}	SO_4^{2-}
SBF	142.0	5.0	2.5	1.5	147.8	4.2	1.0	0.5
Ca-free solution	142.0	5.0	0	1.5	147.8	4.2	1.0	0.5
Human plasma	142.0	5.0	2.5	1.5	103.0	27.0	1.0	0.5

[1] Cerac, USA.
[2] JT Baker, USA.
[3] Allied Chemical, USA.

3. Results

Fig. 1 shows the X-ray diffraction patterns of the coating surfaces after different times in SBF. The peaks that appear in the XRD of the starting coatings are due to partial crystallization of the glass during the fabrication procedure (Fig. 1). In all the cases the volume of crystalline phases is below 5 vol% [5]. No appreciable changes occur in the patterns of 6P61 and 6P68 coatings after 2 months in SBF (Fig. 1). After 1 month in SBF the apatite peaks are clearly visible in the X-ray analysis of the 6P57 coatings. The relative intensity of the peaks suggests that the apatite crystals growth preferentially with the *c*-axis perpendicular to the coating.

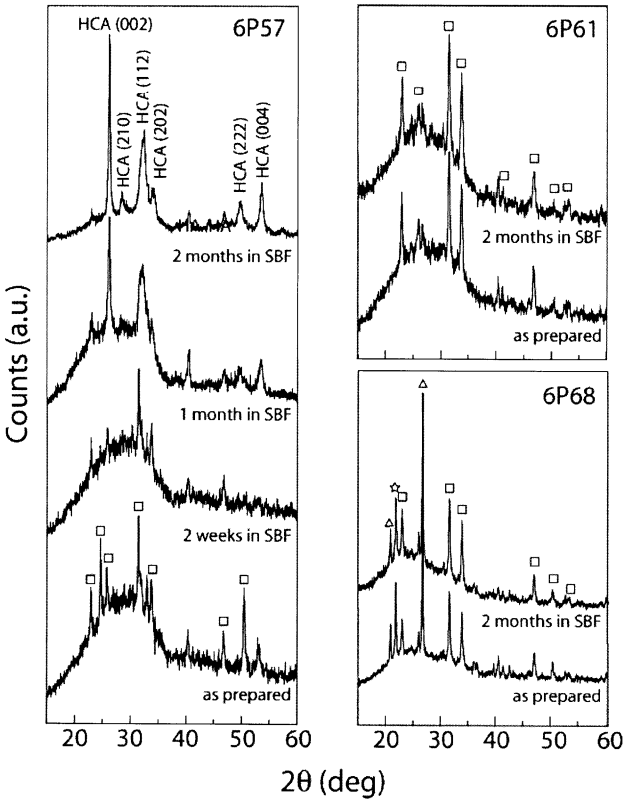

Fig. 1. XRD diffraction patterns of 6P57, 6P61 and 6P68 coatings after immersion in SBF for different times. The main crystalline phases are: $2.4CaO \cdot 0.6Na_2OP_2O_5$ (□); SiO_2, quartz (△); SiO_2, cristobalite (☆); $Ca_{10}(PO_4)_3(CO_3)_3(OH)_2$ carbonated hydroxyapatite,(HCA).

The 6P57 coatings corrode very fast in SBF (Figs. 2 and 3). After 1 day in SBF morphological changes can be clearly observed on the surface of the coatings using AFM (Fig. 2). Cross sectional analyses of the coatings soaked for 2 weeks show three separate regions (Fig. 4): a layer of the remaining glass in contact with the metal; a surface layer rich in silica with small amounts of Ca, P and Al; and a Si-rich layer between them. After 1 month in SBF the surface layer disappears and is substituted by a $\sim 5\,\mu m$ thick layer of HCA that grows on the Si-rich surface (Fig. 5). The apatite crystals were detected by XRD (Fig. 1) and they completely cover the coating surface (Fig. 6). This behavior was similar for the samples immersed in 20 or 200 ml of SBF. The apatite crystals have flake-like morphology with sizes in the range of 50–100 nm. In the analysis of the apatite precipitates using FTIRSM (Fig. 5) the P–O peak at $\sim 510\,m^{-1}$ and the C–O shoulder at $\sim 950\,cm^{-1}$ (that corresponds to the C–O vibration mode in CO_3^{2-}) were consistent with carbonated hydroxyapatite (HCA, $Ca_{10}(PO_4)_3(CO_3)_3(OH)_2$) [8,10]. The calibrated EDS analysis indicates that the apatite incorporates 1–5 wt% MgO in its structure. No other elements could be detected in the precipitated apatite by EDS or XPS. The precipitation of HCA was accompanied by a decrease in the Ca and P concentrations in SBF (Fig. 7). The apatite layer grew to a thickness of $\sim 20\,\mu m$ in the samples soaked for 2 months (Fig. 8). The composition and structure of the glass layer that remained attached to the metal were the same as the original 6P57 coating (Figs. 5 and 8). Leaching of Si into the solution continued at a constant linear rate even after the precipitation of HCA. No apatite precipitated on the coatings immersed in the solution without calcium.

The coatings prepared using 6P61 and 6P68 glasses are much more resistant to corrosion in SBF (Figs. 3 and 8). No corrosion or variation in the coating composition could be observed in the coatings' cross

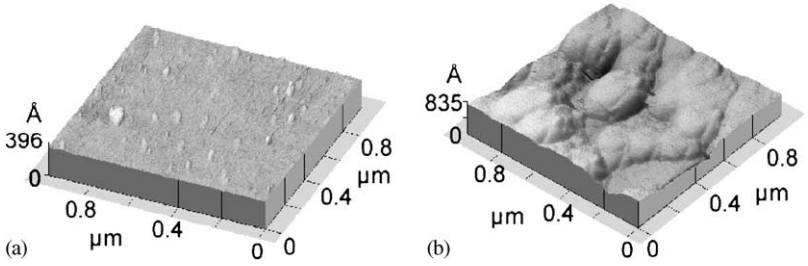

Fig. 2. AFM scans of the surface of a 6P57 after firing (a) and after 1 day in SBF (b), showing the morphological change during the early stages of glass dissolution.

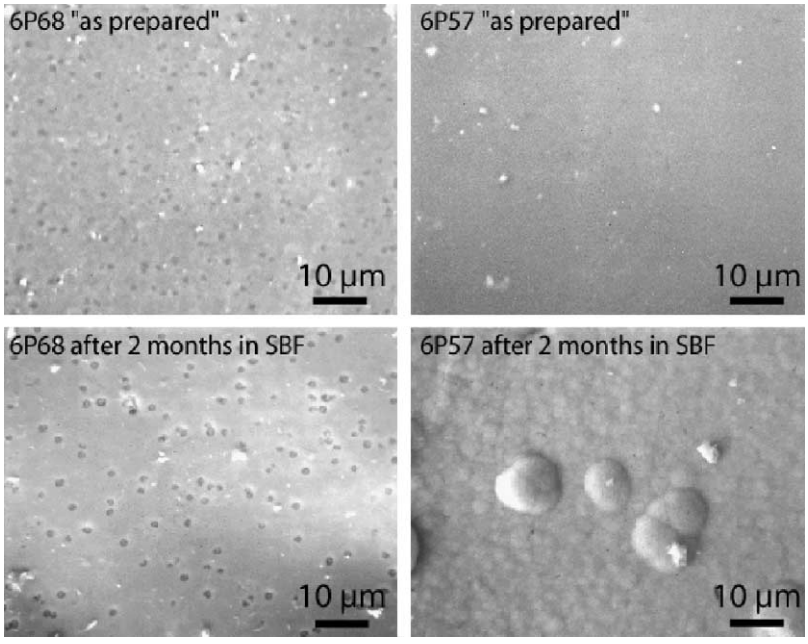

Fig. 3. SEM micrographs of the surface of 6P57 and 6P68 coatings after soaking in SBF. The surface of 6P68 coatings remains unaltered even after 2 months whereas apatite has precipitated in 6P57.

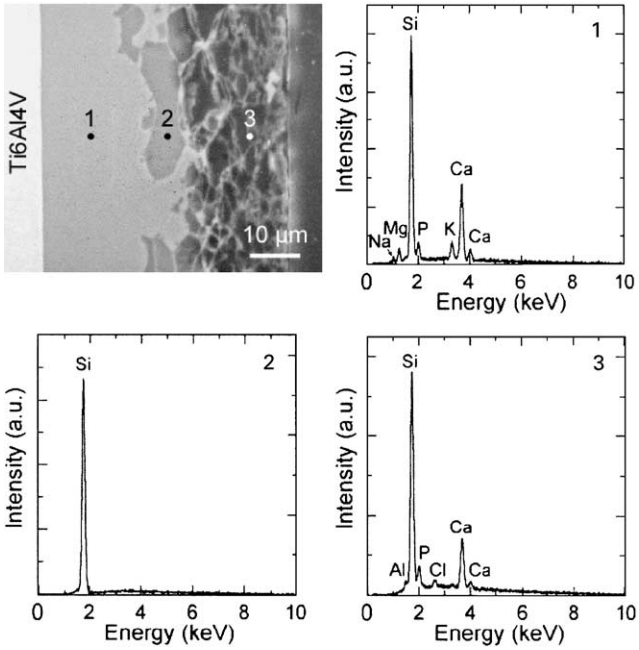

Fig. 4. SEM and associated EDS analysis of the cross section of a 6P57 coating after 2 weeks in SBF. The Cl peak on the surface layer is due to infiltration of the mounting resin.

sections using SEM and EDS elemental line profiles even after soaking for 2 months in SBF. For 6P61 coatings, the leaching of silica into SBF is more than ten times slower than for 6P57. After 2 months no measurable increase in the Si content was observed in the solution containing 6P67 coatings.

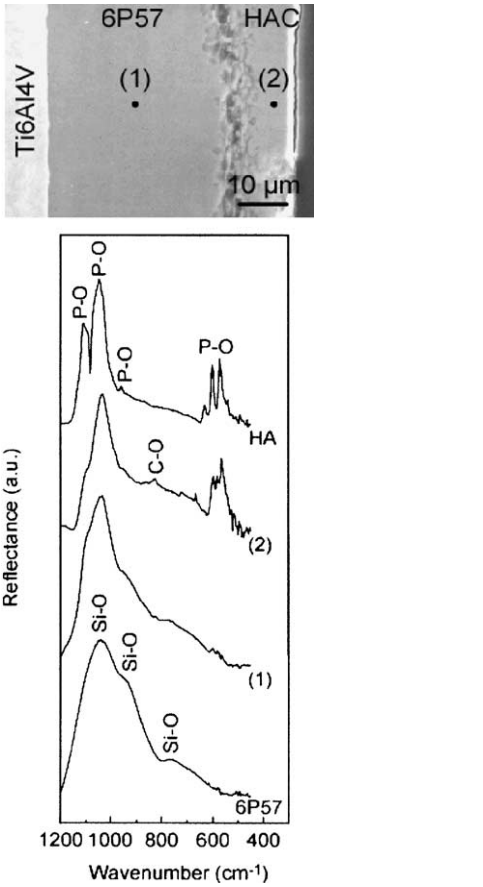

Fig. 5. Cross section of a 6P57 coating after 1 month in SBF. FTIRSM of selected points is also presented. A layer of the original glass remains attached to the metal. The P–O and C–O bands on the FTIRSM analysis of the top layer are consistent with hydroxycarbonate apatite.

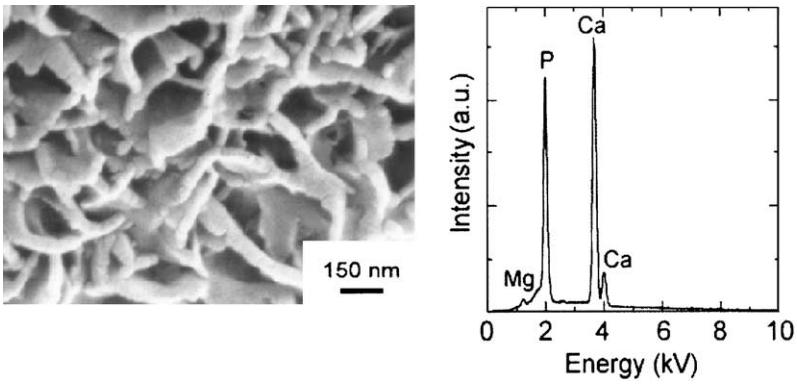

Fig. 6. SEM image and associated EDS analysis of the apatite crystals precipitated on 6P57 after 2 months in SBF. The crystals contain 1–5 wt% MgO.

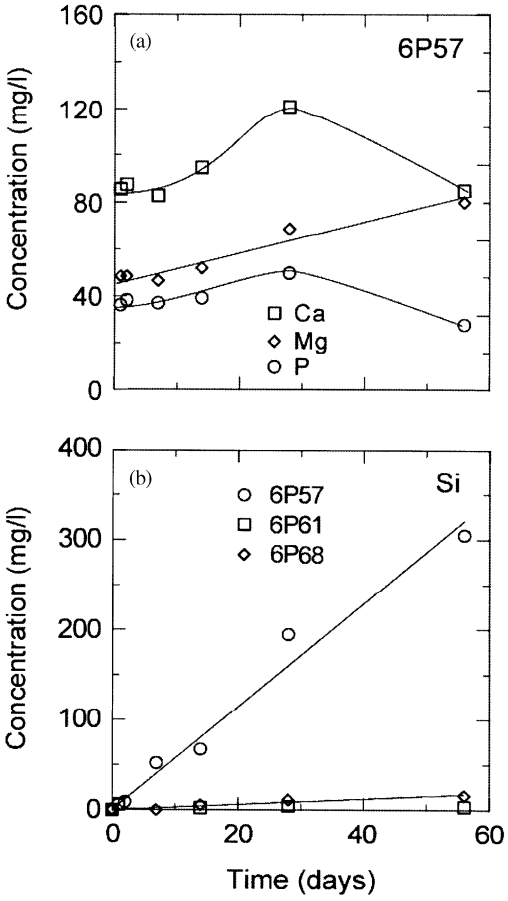

Fig. 7. Evolution of Ca–P and Si concentrations in SBF. The decrease of the Ca and P concentrations in the solution containing 6P57 coatings coincides with the precipitation of HCA. The leaching of silica continues at a linear constant rate in 6P57 coatings even after 2 months in SBF. There is not a measurable increase in the Si concentration of the solution containing 6P68 coatings.

The corrosion of the 6P57 coatings is not homogeneous. In some areas the coating has corroded all the way down to the glass/metal interface after 2 weeks in SBF (Fig. 9). This resulted in the formation of cracks that after 2 months reached the glass/metal interface and initiated delamination (Fig. 10). No cracks were observed on 6P61 and 6P67 coatings. The indentation cracks placed on the 6P57 coatings grew during immersion in SBF with decreasing velocities of 10^{-10} m/s or lower, up to the lengths of $\sim$200 μm (Fig. 11). No appreciable crack growth occurred on the other coatings or on the 6P57 coatings placed in dehydrated oil.

During the indentation tests performed at the glass/metal interface after immersion in SBF the cracks do not propagate along the interface but rather tend to be driven into the glass as seen with the original coatings before the in vitro tests [5,6].

4. Discussion

The in vitro response of the coatings depends strongly on their composition, in particular on their silica content. The observed behavior is similar to that reported for bulk glasses in the SiO_2–Na_2O–CaO–P_2O_5 system (which includes Bioglass®), and other related compositions [11–18]. Low silica compositions have a more open network structure that facilitates ion exchange with the solution, resulting in faster glass corrosion and precipitation of apatite. In the coatings studied here, the critical silica content was around 60 wt%. A layer of carbonated apatite grew in vitro on the surface of the coatings with lower silica content (6P57) (Fig. 5) whereas coatings with higher silica content were more resistant to corrosion and did not form apatite. The HCA layer grew with time with the crystalline *c*-axis preferentially oriented perpendicular to the coating surface as observed for bulk bioactive glasses [19].

The analysis of the coating behavior in SBF is consistent with a mechanism of apatite formation similar to that described by Hench for Bioglass® [13]. The steps involved are: the exchange of Na^+ and K^+

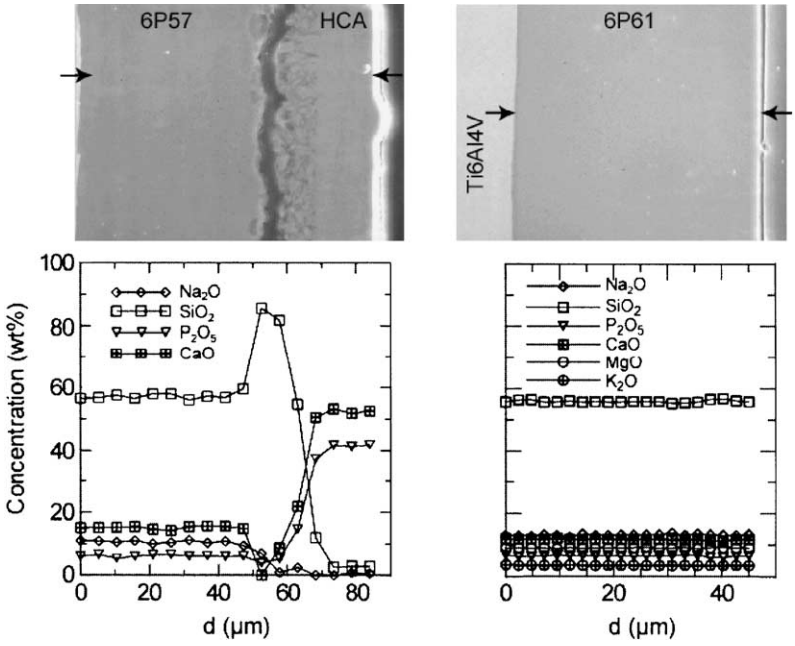

Fig. 8. Elemental cross section analysis (SEM-EDS) of 6P57 and 6P61 coatings after 2 months in SBF. A ~20 μm thick apatite layer is visible on the 6P57 coating surface growing on a Si-rich region. No appreciable changes can be observed on the 6P61 coatings.

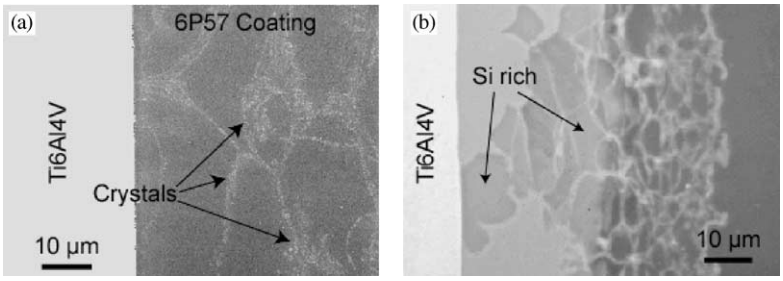

Fig. 9. (a) SEM image of a 6P57 coating, after etching for 5 s with 5 vol% HFl the crystallization in the glass is visible; (b) inhomogeneous corrosion in a 6P57 coating after 2 weeks in SBF.

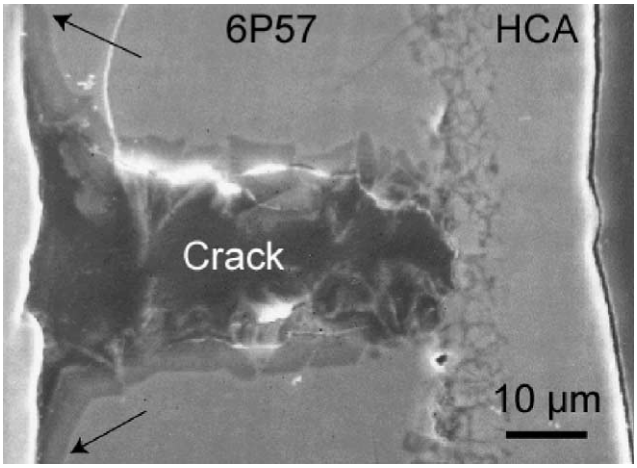

Fig. 10. Crack formed in the 6P57 coating after 2 months in SBF. The crack has reached the interface and initiated delamination.

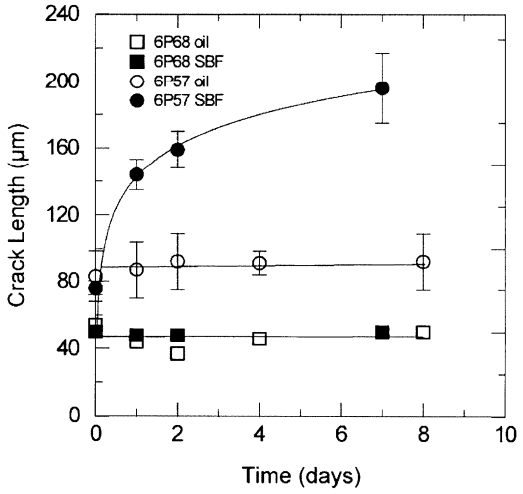

Fig. 11. Growth of indentation cracks on 6P57 and 6P68 coatings in SBF and dehydrated mineral oil. On the 6P57 coatings in SBF the crack grows with decreasing velocity as it moves away from the indentation stress field.

from the glass with H^+ or H_3O^+ from solution, accompanied by the loss of soluble silica into the solution and the formation of silanols on the glass surface; condensation and repolymerization of a SiO_2-rich layer on the surface; migration of Ca^{2+} and PO_4^{3-} through the silica-rich layer forming a $CaO–P_2O_5$-rich film that incorporates calcium and phosphates from solution; finally, the crystallization of the amorphous calcium phosphate film to form an apatite layer. De Aza et al. [20] have pointed out that the increase in pH on the glass surface due to the ionic exchange between the labile cations Na^+, K^+, Ca^+, etc., is necessary for the partial dissolution of the silica-rich layer and the subsequent apatite precipitation. The observed dissolution of silica into SBF (Fig. 7) during the in vitro tests of 6P57 coatings is consistent with the observation of De Aza et al. [20] that the high local pH attained at the bioactive glass/SBF interface promotes the partial dissolution of the silica hydrogel layer that forms on the glass surface.

In coatings made from 6P57 glasses that were immersed for 2 weeks in SBF the formation of a silica-rich layer, $\sim$10 μm thick, containing also Ca and P can be observed (Fig. 4). This agrees with the sequence proposed by Hench in which a silica-rich layer forms on the surface, through which the Ca and P species migrate. The presence of Al traces in this layer also was observed on the related bulk glasses and can be due to the presence of alumina impurities in the starting oxides used in the glass preparation. Even though alumina additions at levels higher than 7.5 wt% have been reported to reduce the bone bonding ability of bioactive glasses [21] the low levels found here (the Al_2O_3 could not be detected on the starting coatings using EDS) did not inhibit apatite precipitation. This is in agreement with the studies of the effect of Al_2O_3 in bioactive glasses published by Ohura et al. [22] and Andersson et al. [23].

The initial increase in the Ca, P, and Mg concentrations observed in the SBF containing 6P57 coatings (Fig. 7) is due to the ionic exchange with the glass. After 1 month the precipitation of apatite on the glass surface resulted in the observed decrease of the Ca and P concentrations. It should be noted that the apatite layer is porous (Fig. 3) and does not protect the coating from corrosion in SBF, confirmed by the constant leaching of Si (Fig. 7). The overall process of leaching and HCA formation was slower in the coatings than in the Bioglass® due to their higher silica content that resulted in a more compact glass structure. However, the formation of apatite was independent of the amount of SBF used in the test (from 20 to 200 ml), as expected if the apatite precipitates after a process similar to that described by Hench, and not because of saturation of the solution with Ca and P from the glass. Regina et al. [8] have pointed out that the presence of calcium and phosphorus in solution accelerates the precipitation of hydroxyapatite. Our results suggest that the high silica glasses used in the coatings require Ca in the solution for the formation of HCA, due to their slower ionic exchange rate.

MgO and K_2O were added to the glasses in order to adjust their thermal expansions and softening points such that enameling could be carried out at temperatures below the $\alpha \rightarrow \beta$ transformation of Ti in the alloy (955–1010°C), without generating large thermal stresses. [5] The work of Brink et al. [12] suggests that small amounts of K_2O and MgO do not affect bioactivity of glasses, however, there have been reports that Mg inhibits the precipitation of hydroxyapatite [8,9,24]. Our results indicated that coatings containing as much as 8.5 wt% of MgO and 56.5 wt% of SiO_2 precipitated apatite during the in vitro tests. The precipitated apatite incorporates 1–5 wt% MgO into its structure. The lack of MgO on the surface layer of the coatings immersed for 2 weeks in SBF suggests that the magnesium is coming from the solution. However, there has not been a report of magnesium present on the apatite precipitated on the surface of MgO-free glasses.

The small amount of crystallization that occurs during the firing of the coatings does not compromise the ability of the glass to form HCA. Crystallization and inhomogenities in the initial coating can be the cause of the non-uniform leaching of glass elements into the solution. As a result, the amorphous SiO_2-rich layer that forms at intermediate times is not continuous and can reach the glass/metal interface in some areas (Figs. 4 and 9).

A simple elastic analysis for 50 μm coatings on Ti6Al4V predicts tensile stresses of $\sim$50 and 25 MPa, for 6P57 and 6P61, respectively, and compressive stresses of $\sim$–25 MPa for 6P68 [5].

In 6P57 coatings, these stresses could be high enough to drive the slow growth of cracks in SBF. Crack formation can be detrimental for the long-term stability of the coating, since the cracks eventually reach the interface and initiate delamination. The precipitation of a hydroxyapatite layer on the coating surface does not shield the crack from the solution and it continues growing (Fig. 10). Because of the lower stresses and higher resistance to corrosion, cracks did not grow in the 6P61 and 6P68 coatings. The results of the indentation tests qualitatively agree with these observations. In 6P68 coatings the compressive residual stresses effectively arrest the growth of indentation cracks. However, in the 6P57 coatings in SBF the crack growth is driven by the combined stresses from the thermal expansion mismatch and the indentation field. As the cracks grow away from the indentation stress field, the overall stresses decrease and the cracks decelerate. Typically, the indentation stress field decreases significantly at distances greater than the indent size ($\sim$40 μm). Accordingly, the results (Fig. 11) indicate

an upper limit for the crack velocity in SBF under the thermal stresses of $\sim 10^{-10}$ m/s. After 7–8 days the corrosion of the 6P57 surface hampered the measurement of the crack length. The cracks did not grow on the 6P57 coatings in dehydrated mineral oil, emphasizing the role of SBF on the corrosion of the glass.

As expected, immersion in SBF did not affect the adhesion of the interfaces that were not in contact with the solution. During the indentations at the glass/metal interfaces after the in vitro tests, the cracks did not propagate along the interface, but rather tended to be driven into the glass as seen in the original coatings [5,6].

5. Conclusions

The in vitro behavior of the silicate glass coatings analyzed in this work is similar to that of bulk glasses. Coatings with silica content lower than 60 wt% precipitated apatite during in vitro testing. The mechanism of apatite formation is similar to that described by Hench for Bioglass®. However, due to their lower silica content, the thermal expansion of these coatings is higher than that of Ti and the tensile thermal stresses generated during processing drove the slow growth of cracks in SBF. The cracks eventually reached the interface and initiated delamination.

Higher silica coatings did not form apatite but were more resistant to corrosion and slow crack growth. At the moment, graded coatings that have glasses with high silica content in contact with the metal and a low silica glass on their surface are under development in order to improve their long term stability while maintaining a good biological response.

Acknowledgements

This work was supported by the NIH/NIDCR grant 1R01DE11289. Jose M. Gomez-Vega wishes to thank the Spanish Ministry of Education (MEC) for financial support. The Advanced Light Source is supported by the Director, Office of Science, Office of Basic Energy Sciences, Materials Sciences Division, of the US Department of Energy under Contract No. DE-AC03-76SF00098 at Lawrence Berkeley National Laboratory.

References

[1] Hench LL, Andersoon O. Bioactive glass coatings. In: Hench LL, Wilson J, editors. An introduction to bioceramics. New Jersey: World Scientific, 1993. p. 239–60.
[2] Sousa SR, Barbosa MA. Electrochemistry of AISI-316L stainless steel in calcium phosphate and protein solutions. J Mater Sci 1991;2:19–26.
[3] Sousa SR, Barbosa MA. The effect of hydroxyapatite thickness on metal ion release from stainless steel substrates. J Mater Sci 1995;6:818–23.
[4] Sousa SR, Barbosa MA. Effect of hydroxyapatite thickness on metal ion release from Ti6Al4V substrates. Biomaterials 1996;17:397–404.
[5] Gomez-Vega JM, Saiz E, Tomsia AP. Glass-based coatings for titanium implant alloys. J Biomed Mater Res 1999;46:549–59.
[6] Pazo A, Saiz E, Tomsia AP. Silicate glass coatings on Ti-based implants. Acta Mater 1998;46:2551–8.
[7] Pazo A, Saiz E, Tomsia AP. Bioactive coatings on Ti and Ti6Al4V alloys for medical applications. In: Tomsia AP, Glaeser AM, editors. Ceramic microstructures: control at the atomic level. Berkeley: Plenum Press, 1998. p. 543–50.
[8] Regina M, Filgueiras MRT, Latorre G, Hench LL. Solution effects on the surface reactions of three bioactive glass compositions. J Biomed Mater Res 1993;27:1485–93.
[9] Ebisawa Y, Kokubo T, Ohura K, Yamamuro T. Bioactivity of $CaOSiO_2$-based glasses—In vitro evaluation. J Mater Sci 1990;1:239–44.
[10] Nelson DGA, Featherstone JDB. Preparation, analysis, and characterization of carbonated apatites. Calcified Tissue Intl 1982;34:S69–81.
[11] Ogino M, Hench LL. Formation of calcium phosphate films on silicate glasses. J Non-Crys Sol 1980;38&39:673–8.
[12] Brink M, Turunen T, Happonen RP, Yli-Urpo A. Compositional dependence of bioactivity of glasses in the system Na_2O–K_2O–MgO–CaO–B_2O_3–P_2O_5–SiO_2. J Biomed Mater Res 1997;37:114–21.
[13] Hench LL. Bioceramics: from concept to clinic. J Am Ceram Soc 1991;74:1487–570.
[14] Kim CY, Clark AE, Hench LL. Early stages of calcium phosphate layer formation in bioglasses. J Non-Crys Sol 1989;113:195–202.
[15] Kim CY, Clark AE, Hench LL. Compositional dependence of calcium phosphate layer formation in fluoride bioglasses. J Biomed Mater Res 1992;26:1147–61.
[16] Ogino M, Ohuchi F, Hench LL. Compositional dependence of the formation of calcium phosphate films on bioglass. J Biomed Mater Res 1980;15:55–64.
[17] Lockyer MWG, Holland D, Dupree R. NMR investigation of the structure of some bioactive and related glasses. J Non-Crys Sol 1995;188:207–19.
[18] Hill R. An alternative view of the degradation of bioglass. J Mater Sci Lett 1996;15:1122–5.
[19] Rehman I, Knowles JC, Bonfield W. Analysis of in vitro reaction layers formed on Bioglass(R) using thin- film X-ray diffraction and ATR-FTIR microspectroscopy. J Biomed Mater Res 1998;41:162–6.
[20] de Aza PN, Guitian F, Merlos A, Loratamayo E, de Aza S. Bioceramics—simulated body fluid interfaces—pH and its influence of hydroxyapatite formation. J Mater Sci 1996;7:399–402.
[21] Gross U, Kinne R, Schmitz HJ, Strunz V. The response of bone to surface active glass/glass–ceramics. In: Williams DF, editor. CRC critical reviews in biocompatibility. Boca Raton: CRC Press, 1988. p. 2.
[22] Ohura K, Nakamura T, Yamamuro T, Ebisawa Y, Kokubo T, Kotoura Y, Oka M. Bioactivity of CaO SiO_2 glasses added with various ions. J Mater Sci 1992;3:95–100.
[23] Andersson OH, Karlsson KH, Kangasniemi K, Yli- Urpo A. Models for physical properties and bioactivity of phosphate opal glasses. Glastech Ber 1988;61:300–5.
[24] Li P, Ohtsuki C, Kokubo T, Nakanishi K, Soga N, Nakamura T, Yamamuro T. Effects of ions in aqueous media on hydroxyapatite induction by silica gel and its relevance to bioactivity of bioactive glasses and glass-ceramics. J Appl Biomater 1993;4:221–9.